

Conformational Changes of the Nucleotide Site of the Plasma Membrane Ca^{2+} -ATPase Probed by Fluorescence Quenching[†]

Mirian M. Fonseca, Helena M. Scofano, Paulo C. Carvalho-Alves, Hector Barrabin, and Julio A. Mignaco*

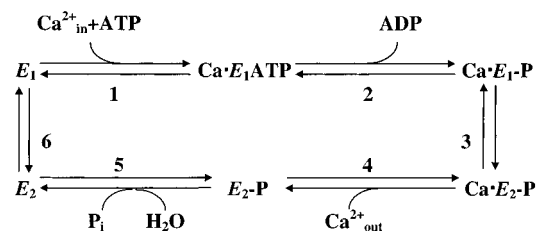
Departamento de Bioquímica Médica, ICB/CCS, Universidade Federal do Rio de Janeiro, Cidade Universitária, CEP 21941-590, Rio de Janeiro, RJ, Brazil

Received September 19, 2001; Revised Manuscript Received April 16, 2002

ABSTRACT: Fluorescence quenching by the water-soluble ions I^- and Cs^+ was used to probe solvent accessibility and polarity of the nucleotide/fluorescein isothiocyanate binding pocket of the purified soluble Ca^{2+} -ATPase from plasma membranes. The $\text{E}_1\cdot\text{Ca}\cdot\text{CaM}$ conformer was the least accessible state studied, presenting the lowest suppression constant (K_q) for both I^- ($K_q = 6.7 \text{ M}^{-1}$) and Cs^+ ($K_q = 0.7 \text{ M}^{-1}$). Accessibility to I^- was similar for the $\text{E}_2\cdot\text{VO}_4$ and $\text{E}_1\cdot\text{Ca}$ states ($K_q = 7.13$ and 7.5 M^{-1} , respectively), whereas E_2 was slightly more accessible ($K_q = 9.1 \text{ M}^{-1}$). The phosphorylated state $\text{E}_2\text{-P}$ presented the highest accessibility, with a K_q of 16.5 M^{-1} , very near the K_q of 20.3 M^{-1} for free FITC. I^- was unequivocally a better fluorescence quencher, being usually nearly 3-fold as efficient as Cs^+ , as indicated by the $K_q(\text{I}^-)/K_q(\text{Cs}^+)$ ratio (R_q). The advent of a positive charge cluster on the nucleotide/fluorescein binding pocket in different states was suggested by the increase in R_q , which reached a value as high as 9.5 for the $\text{E}_1\cdot\text{Ca}\cdot\text{CaM}$ conformer. These results indicate (i) a very high water accessibility of the nucleotide/fluorescein pocket for $\text{E}_2\text{-P}$ that (ii) is more restricted on the free E_2 state and (iii) becomes rather lower for the $\text{E}_1\cdot\text{Ca}$ states. Additionally, a positive charge effect of amino acids on the nucleotide site, possibly related to ATP binding and phosphoryl transfer, appears in these $\text{E}_1\cdot\text{Ca}$ states, being absent in the phosphorylated and nonphosphorylated E_2 states.

The plasma membrane Ca^{2+} -ATPase (PMCA¹) is a P-type ATPase present in all studied eukaryotic cells and is ultimately responsible for fine-tuning the internal Ca^{2+} concentrations needed for cell survival. In mammals, this enzyme is found as four major isoforms (PMCA1–4), which are differentially expressed in tissues. This number can be further increased by alternative splicing (1, 2). PMCA shows a high stringency for ATP as the energy donor for Ca^{2+} transport and shuttles one Ca^{2+} ion to the extracellular side for each hydrolysis cycle (3, 4). Major modulators of these enzyme's activities are calmodulin (CaM), acidic phospholipids and fatty acids (5, 6), Ca^{2+} itself, oligomerization (7, 8), in vivo proteolysis by calpain (or trypsin in vitro; 9, 10), and phosphorylation by PKA and PKC (11–13). On the basis of kinetic data and by analogy with its sarcoplasmic reticulum counterpart, a simplified transport scheme proposes that the enzyme cycles through two major conformational states, namely, E_1 and E_2 (Scheme 1). These states are clearly distinct in reference to their affinity for Ca^{2+} ($\text{E}_1 \gg \text{E}_2$)

Scheme 1. Catalytic Cycle Proposed for the Plasma Membrane Ca^{2+} -ATPase



and their ability to be phosphorylated by ATP (E_1) or inorganic phosphate (E_2) (14, 15). Resolution of the amino acid sequence of the enzyme has been useful for modeling secondary and tertiary structures and identifying important residues (2). However, a global perception of the changes that the nucleotide site of the enzyme undergoes during the catalytic cycle is missing due to the lack of the high amounts of purified enzyme needed for structural approaches. In this study, this apparent difficulty was circumvented by attaching fluorescein isothiocyanate (FITC) to a lysine residue (Lys-591; 16) located within or in the immediate vicinity of the catalytic nucleotide site of the PMCA and then following the accessibility of fluorescence quenchers to this probe in the presence of different ligands. Our data indicate that the catalytic site of PMCA bears significant conformational/hydrophobicity/polarity changes, and thus solvent accessibility differs widely among the various states found during the catalytic cycle.

[†] This work was supported by grants from Financiadora de Estudos e Projetos (FINEP), Conselho Nacional de Desenvolvimento Científico e Tecnológico (CNPq), PRONEX (Convênio 76.97.1000.00), and Fundação de Amparo à Pesquisa do Estado do Rio de Janeiro (FAPERJ).

* Corresponding author [fax (+55)-21-2270-8647; e-mail jmignaco@bioqmed.ufrj.br].

¹ Abbreviations: PMCA, plasma membrane Ca^{2+} -ATPase; CaM, calmodulin; FITC, fluorescein isothiocyanate; FITC-PMCA, FITC-labeled purified PMCA; K_q , fluorescence suppression constant; R_q , ratio of the K_q values for I^- and Cs^+ ; SERCA, sarco-endoplasmic reticulum Ca^{2+} -ATPase.

EXPERIMENTAL PROCEDURES

Reagents. FITC, pNPP (dicyclohexylammonium salt), ATP (disodium salt), EGTA, MOPS, Tris, and CaM were from Sigma. CaM-Sepharose 4B was from Pharmacia. All other reagents and buffers were of analytical grade. [γ - 32 P]ATP was synthesized according to the procedure of Walseth and Johnson (17), with [32 P]P_i purchased from the Instituto de Pesquisas Energéticas e Nucleares (IPEN-SP/Brazil).

Purification of PMCA. Pig erythrocyte ghosts were prepared according to the method of Rega et al. (18). PMCA was solubilized and purified by a Sepharose-4B-calmodulin affinity chromatography, as described by Caroni et al. (19) and modified by Pasa et al. (20). Protein concentration was determined according to the method of Lowry et al. (21) (ghosts) or Peterson (22) (purified PMCA). Purified soluble enzyme was used throughout this paper.

Labeling of PMCA with FITC. Ghosts (18 mL at 4 mg/mL) were incubated in a medium containing 20 μ M FITC, 10 mM BTP-Cl (pH 7.4), and no added Ca²⁺, in a dark shell at room temperature. After 40 min, the sample was pelleted for 10 min at 20000g, resuspended to 18 mL with 100 mM Tris-Cl (pH 7.4), repelleted, and resuspended again two times, and the last pellet was dissolved in the solubilization medium described by Caroni et al. (19), with 0.2 μ M lysine added to further deplete residual FITC. The rest of the purification procedure was as stated by those authors. FITC solutions were always freshly made to 1 mM in ethanol prior to labeling. Nonlabeled PMCA purifications were always run in parallel in order to have quasi-similar unlabeled PMCA as hydrolase and fluorescence controls.

Assessment of Labeling with FITC. Labeling was assessed by comparison of the ratios of inactivation of the ATPase and pNPPase activities and by measuring the light absorption and fluorescence of the labeled purified PMCA. The ratio of bound FITC per protein molecule was calculated by dividing the FITC concentration (obtained by optical density of purified FITC-PMCA, using $\epsilon^{492} = 68000 \text{ M}^{-1}$ in water, at pH 7.0) by the protein concentration and was double-checked by the fluorescence of FITC-PMCA, plotted against a standard curve (in arbitrary units) generated with free fluorescein. The labeling ratio averaged 0.90 mol of FITC/mol of PMCA. Labeling was fully prevented by the addition of 3 mM ATP to the labeling medium.

ATPase and pNPPase Activities. ATPase activity was assayed for each paired preparation in 0.2 mL of medium containing 30 mM Tris-Cl (pH 7.0), 120 mM KCl, 5.5 mM MgCl₂, 0.2 mM EGTA, 10 μ M free Ca²⁺, 1 mM [γ - 32 P]-ATP, and 2 μ g/mL PMCA or FITC-PMCA. Reactions were quenched after 60 min at 37 °C by the addition of 0.1 mL of 0.1 N HCl, followed by 0.2 mL of activated charcoal in 0.1 N HCl and spinning for 5 min \times 10000 rpm in an Eppendorf centrifuge. The supernatant containing the [32 P]-P_i released was counted by liquid scintillation (23). The ATPase activity of ghosts was assayed as above, however, with 1 mM ouabain and 0.2 mg/mL ghost protein in place of purified PMCA. pNPP hydrolysis was measured continuously by the release of pNP in a GBC Cintra-20 spectrophotometer, set at 425 nm. The medium was essentially as above, except that 13 mM pNPP substituted for ATP and small amounts of CaCl₂ were sequentially added to give different free Ca²⁺. The CaCl₂ needed was calculated for

each Ca²⁺ by use of a computer program (24) derived from the original by Fabiato and Fabiato (25) and using the Schwartzbach (26) constant for dissociation of the Ca-EGTA complex.

Fluorescence of FITC-PMCA. Fluorescence of the labeled, purified enzyme was measured in a Hitachi F4500 spectrofluorometer. The spectrum and yield of labeling were determined with excitation set at 480 nm and emission scanning from 500 to 600 nm. For quenching experiments, as well as for measurements of fluorescence levels, the emission was continuously recorded at 520 nm, and values were corrected against the column elution buffer and for dilution effects. The fluorescence at 520 nm and the spectrum of FITC were not directly modified by the addition of EGTA, Ca²⁺, and/or P_i to the samples (not shown).

Fluorescence Quenching. Two fluorescence quenchers with opposite charges were used, KI and CsCl. Standard suppression media contained 2 μ g/mL purified soluble FITC-PMCA, 10 mM MgCl₂, 80 mM MOPS-OH (pH 7.4), 120 mM KCl, and 0.5 mM EGTA, in a final volume of 0.5 mL. The concentrated quenchers (1–5 μ L) were sequentially added, and fluorescence was recorded for 3 min. Changes to this medium included CaCl₂ to give different free Ca²⁺, CaM, sodium orthovanadate, buffered sodium phosphate, and native or denatured enzyme. The final concentration of detergent and lipids in the samples varied from 0.0008 to 0.0012% C₁₂E₈ and from 3.3 to 5.0 μ g \cdot mL⁻¹ and presented no influence on the quenching constants observed. The enzyme is stable in the suppression medium for at least 1 h. The quenching constants (K_q) were calculated using the Stern–Volmer equation

$$F_0/F = 1 + K_q[Q]$$

(27), where K_q = the Stern–Volmer quenching constant, F_0 = the fluorescence in the absence of quencher, F = the fluorescence in the presence of quencher, and $[Q]$ = the molar concentration of quencher. All of the calculated K_q values were analyzed with Student's t test, with $P < 0.05$ for paired data. The data presented are averages of measurements of no less than eight different experiments, done with at least five different preparations.

Fluorescence Lifetime Determinations. The lifetimes of FITC-PMCA were determined by time-correlated single-photon counting (TCSPC) using an OB920 fluorescence lifetime spectrometer (Edinburgh Analytical Instruments). The determinations were done in quadruplicate or duplicate, and estimates were done using single- and double-exponential decay fitting. In all cases, the decays were adequately fitted by a single-exponential decay.

RESULTS

For most P-type ATPases, labeling with FITC impairs nucleotide binding and ATPase activity, although it does not impair smaller substrates hydrolysis (like pNPP) or phosphorylation by P_i (28, 29). For PMCA, however, pNPP hydrolysis is known to be partially impaired by this labeling (30). The molecular reasons for such differences are not clear at this moment and suggest a closer contact between the nucleotide binding domain and the residues on the catalytic site of the PMCA. Accordingly, our FITC-PMCA ATPase activity is usually inhibited in excess of 90%, whereas pNPP

Table 1: K_q Values for KI or CsCl as Quenchers of the Fluorescence of FITC-PMCA^a

	FITC	DFP	EGTA	Ca^{2+}	$\text{Ca}^{2+} + \text{CaM}$	VO_4	$\text{P}_i + \text{DFP}$
KI	20.3 ± 1.7 (10)	12.4 ± 0.8 (14)	9.1 ± 0.5 (20)	7.5 ± 0.8 (22)	6.7 ± 0.7 (25)	7.1 ± 0.5 (8)	13.3 ± 1.3 (10)
CsCl	8.1 ± 0.3 (12)	3.8 ± 0.1 (20)	2.5 ± 0.1 (24)	1.2 ± 0.3 (24)	0.7 ± 0.02 (27)	1.5 ± 0.07 (10)	4.2 ± 0.5 (14)
R_q	2.5 ± 0.2	3.3 ± 0.2	3.6 ± 0.2	6.3 ± 1.7	9.6 ± 1.0	4.7 ± 0.4	3.2 ± 0.5

^a Values for K_q are expressed as M^{-1} . Data are presented as mean \pm SD. Number of experiments is in parentheses. R_q is the ratio $K_q(\text{I}^-)/K_q(\text{Cs}^+)$. FITC, free FITC; DFP, Gdm-Cl denatured FITC-PMCA.

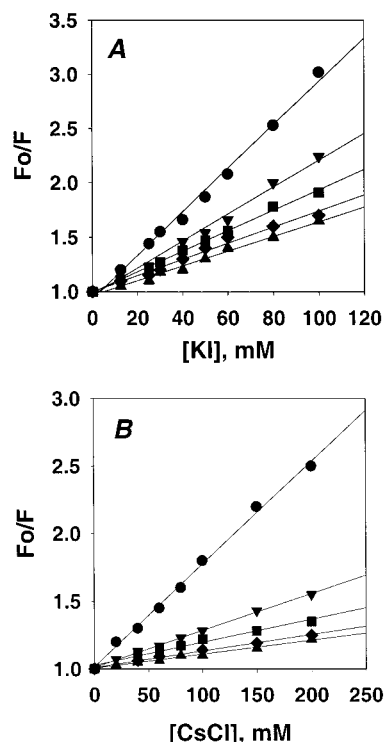


FIGURE 1: Fluorescence quenching of FITC-PMCA by iodide (A) or cesium (B). The curves represent the relative quenching obtained for free FITC (●), Gdm-Cl denatured FITC-PMCA (▼), or native FITC-PMCA in the presence of 0.5 mM EGTA (■), 1 mM Ca^{2+} (◆), or 10 μM Ca^{2+} + 2 $\mu\text{g}/\text{mL}$ CaM (▲). The media also contained 80 mM MOPS-Tris (pH 7.4), 120 mM KCl, and 10 mM MgCl_2 .

hydrolysis is preserved by $>50\%$ (not shown). No relevant differences are observed for the Ca^{2+} dependence of the basal and CaM-stimulated remaining pNPPase activity when unlabeled PMCA and FITC-PMCA are compared (not shown), suggesting that FITC-modified PMCA retains native properties with respect to Ca^{2+} and CaM binding sites and a protein structure relevant to the hydrolysis of substrate.

The fluorescence emission spectrum of FITC-PMCA appears to be very similar to that of free FITC, presenting a maximum around 520–522 nm (not shown). The spectral properties of the label are not altered by the addition of enzyme ligands such as Ca^{2+} or phosphate or by Ca^{2+} sequestration by EGTA (not shown). The effects of two fluorescence quenchers (I^- and Cs^+) with opposite charges were tested. The addition of increasing concentrations of both quenchers (not shown) results in a concomitant decrease in FITC-PMCA fluorescence. KI proved to be a better quencher than CsCl, because in all cases the quenching constants (K_q) obtained for KI are significantly larger (Table 1). Figure 1 depicts the quenching behavior for free FITC, FITC-PMCA previously denatured overnight with Gdm-Cl, and “native” FITC-PMCA in the presence of different ligands and consequently different conformational states, when con-

Table 2: Fluorescence Lifetimes of FITC-PMCA in the Presence or Absence of KI or CsCl^a

quenching agent	τ (ns)
none	4.27 ± 0.10 ($n = 4$)
KI, 100 mM	3.99 ± 0.07 ($n = 2$)
CsCl, 200 mM	4.33 ± 0.01 ($n = 2$)

^a Lifetimes were measured in the same experimental conditions used for Figure 2. Values were calculated from the experimental data by fitting with a monoexponential decay, because no real improvement in the χ^2 parameter was obtained by applying a double-exponential decay.

fronted with KI (Figure 1A) or CsCl (Figure 1B). Regardless of the experimental conditions, plotting F_0/F as a function of quencher concentration results in a straight line extrapolating to a value near 1 at zero quencher concentration, indicating that a single class of FITC molecules is accessible to the quenchers. Besides, the ratio of FITC bound per ATPase monomers amounts to roughly 0.90 mol/mol, and FITC labeling is prevented by 3 mM ATP (see Experimental Procedures), suggesting that a single molecule of the fluorophore is bound within the nucleotide site per Ca^{2+} -ATPase.

As expected, higher K_q values (20.3 M^{-1} for KI and 8.1 M^{-1} for CsCl) are obtained for free FITC, because in this case the molecule is fully accessible to solvent and, thus, to quenchers. Noticeably, the K_q values for FITC-PMCA previously denatured with 6 M Gdm-Cl are approximately half those values (12.4 and 3.8 M^{-1} , respectively), suggesting that the enzyme regains some structure upon dilution in the assay medium or that the quencher's access to the fluorophore is shielded by the randomly coiled peptides. When fluorescence quenching of the non-denatured FITC-PMCA was done in the presence of either EGTA (E_2 favored), 1 mM free Ca^{2+} ($\text{E}_1 \cdot \text{Ca}$), or 10 μM Ca^{2+} together with 2 $\mu\text{g}/\text{mL}$ CaM ($\text{E}_1 \cdot \text{Ca} \cdot \text{CaM}$), the K_q values were found to be decreasing for the E_2 ($9.2/2.5 \text{ M}^{-1}$), the $\text{E}_1 \cdot \text{Ca}$ ($7.5/1.2 \text{ M}^{-1}$), and the $\text{E}_1 \cdot \text{Ca} \cdot \text{CaM}$ ($6.7/0.7 \text{ M}^{-1}$) conformers, respectively (see Figure 1A,B and Table 1).

Measurements of lifetimes in the presence of both quenchers, I^- and Cs^+ , indicate a static quenching occurs, with a very small contribution of dynamic quenching in the case of I^- (Table 2). This is unexpected considering that for SERCA, a protein presumably very similar to the PMCA, a purely dynamic quenching was previously reported for I^- at similar high quencher concentrations (31). This remarkable difference suggests that the bound FITC must be quite occluded because no appreciable dynamic component is observed. The invariance of the lifetime with the quencher means the formation of a fluorophore–quencher complex or, more probably (considering that the quenchers used here have opposite charge), that quenchers are confined into a restricted space (“active volume”, see ref 32) very close to the fluorescein moiety. If a quencher (one or more molecules)

exists within this volume at the instant the fluorescein becomes excited, “static” quenching is assumed to occur instantaneously. The static quenching effect will be greater at lower diffusion coefficients of quencher into the protein pocket, where fluorescein probe is bound (32). Thus, changes in K_q will follow variations in the accessibility of quenchers through the protein matrix caused by conformational changes.

The data indicate that FITC tethered to a lysine located within the nucleotide domain of the catalytic site (or its near vicinity) is more accessible to the quenchers in the E_2 conformation, whereas a more closed/unaccessible conformation of the nucleotide site, or a deeper positioning of the Lys-591 residue itself within a cleft, is favored when PMCA changes to the E_1 conformers. The difference observed for the K_q values of the two E_1 states ($E_1\cdot\text{Ca}$ and $E_1\cdot\text{Ca}\cdot\text{CaM}$) with I^- is not significant according to Student’s paired t test ($P > 0.05$). On the other hand, the differences in the quenching constants observed with Cs^+ are found to be significant by this same test and thus point to further small changes between these enzymatic states.

Additional information is obtained from the ratios observed for either quencher at each enzyme conformational state. This parameter, here defined as $R_q = K_q(\text{I}^-)/K_q(\text{Cs}^+)$, has a value of 2.5 for free FITC and 3.2–3.3 for the denatured FITC-PMCA and is increased to 3.6 for E_2 , 6.3 for $E_1\cdot\text{Ca}$, and up to 9.6 for the $E_1\cdot\text{Ca}\cdot\text{CaM}$ state (see Table 1). This ratio is interpreted as follows: the closer R_q is to the value found for the R_q of free FITC, the more the observed values of K_q are free from the influence of charged amino acids situated in the vicinity of the bound FITC. Thus, the high values of R_q in the presence of Ca^{2+} might represent an additional ionic attraction for I^- (or conversely repulsion to Cs^+) induced by the conformational changes as basic amino acids near the FITC molecule become more exposed or clustered for the $E_1\cdot\text{Ca}$ and the $E_1\cdot\text{Ca}\cdot\text{CaM}$ states.

As for other P-type ATPases, the E_2 state of PMCA can become phosphorylated by inorganic phosphate in the millimolar range, in the absence of Ca^{2+} (33). We thus incubated the enzyme in the presence of growing concentrations of P_i , therefore gradually dislocating the equilibrium of the reaction to the phosphorylated state denoted $E_2\text{-P}$. A significant increase in the K_q for both quenchers is found to be induced by phosphorylation of the enzyme (Figure 2A,B and Table 3). Figure 2A represents the direct plot of quenching induced by KI in the presence of increasing concentrations of P_i , thus resulting in higher amounts of the $E_2\text{-P}$ intermediate. Apparently, phosphorylation of the enzyme either results in a more “open” form for the surroundings of the nucleotide site or pushes the FITC tethered to Lys-591 toward a water accessible pocket (Table 3).

When the values for K_q are plotted as a function of $[\text{P}_i]$, a saturating profile is observed. The K_q values for quenching with I^- and Cs^+ (Table 3) attain a maximum value at ~ 10 mM and cannot be significantly increased by a higher P_i concentration in the medium, as depicted in Figure 2B, therefore being coherent with a saturable behavior of the phosphoenzyme. The $K_{0.5}$ observed for the increase in K_q elicited by P_i [1.58 mM for KI (Figure 2B) and 2.63 mM for CsCl (data not shown)] is in the range of the $K_{0.5}$ reported for phosphorylation by P_i of the renal PMCA as extrapolated by measuring ATP– P_i exchange (34) and is also in the range described for the SERCA (35). It must be stressed that the

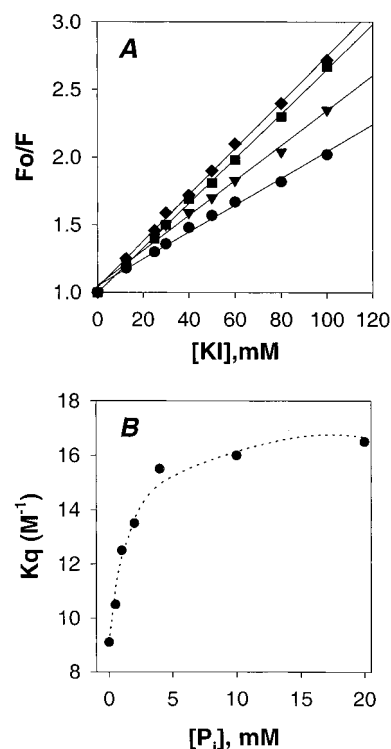


FIGURE 2: Effect of phosphorylation by P_i on the quenching of FITC-PMCA by KI. The experiments were done by increasing the concentration of KI in the presence of different concentrations of P_i . (A) For visualization, only the curves in the presence of 0.5 (\bullet), 2 (\blacktriangledown), 4 (\blacksquare), or 20 mM P_i (\blacklozenge) are represented. (B) K_q values obtained from the experiments in (A) are plotted at each concentration of phosphate. The dotted line represents the fitting obtained with a one-site, ligand binding nonlinear regression. The basic medium was as in Figures 1 and 2.

increase in K_q is observed only for the “native” FITC-PMCA, because controls with Gdm-Cl-denatured enzyme show that the K_q is influenced neither by the increase in ionic force nor by direct interaction of P_i with FITC or the quenchers (data not shown). It is also noteworthy that the maximum K_q values obtained for the phosphorylated FITC-PMCA are higher than the K_q values found for the denatured labeled enzyme.

The relatively high values of K_q for KI (16 M^{-1} ; Figure 2A,B and Table 3) and CsCl (6.5 M^{-1} ; Table 3) observed in the presence of 10 mM P_i , a condition highly favoring the $E_2\text{-P}$ state, can be amply reversed by the addition of 100 μM free Ca^{2+} , with the consequent dephosphorylation and displacement of the equilibrium of the enzyme from the $E_2\text{-P}$ state toward the $E_1\cdot\text{Ca}$ state (see Figure 3 and also Table 3). The K_q values thus obtained (10 M^{-1} for KI and 2.7 M^{-1} for CsCl; Table 3) tend to those observed previously for the FITC-PMCA in the absence of phosphate (Table 1).

A further interesting observation is that the incubation of the enzyme with vanadate does not result in the same K_q values obtained with the addition of P_i . Incubation of the FITC-PMCA with 100 μM orthovanadate, which in our hands is enough to inhibit ATPase activity in excess of 99% (not shown), results in quenching curves less steep than those found for EGTA alone, giving K_q values of 7.1 M^{-1} for KI and 1.5 M^{-1} for CsCl, which are in the same range of the K_q values obtained in the presence of Ca^{2+} alone or $\text{Ca}^{2+} + \text{CaM}$ (Table 1). This was not expected at all, because vanadate is considered to be a phosphate analogue that, yet

Table 3: K_q Values for KI or CsCl as Quenchers of the Fluorescence of FITC-PMCA Incubated with Different Concentrations of P_i ^a

	P_i (mM)							
	none	0.5	1.0	2.0	4.0	10.0	20.0	10.0 + Ca^{2+}
KI	9.1 ± 0.5 (20)	10.5 ± 0.6 (10)	12.5 ± 0.6 (10)	13.5 ± 0.5 (15)	15.5 ± 0.6 (10)	16.0 ± 0.4 (15)	16.5 ± 0.4 (15)	10.0 ± 0.8 (8)
CsCl	2.5 ± 0.1 (24)	3.0 ± 0.3 (12)	3.7 ± 0.4 (12)	4.4 ± 0.5 (16)	5.6 ± 0.4 (12)	6.0 ± 0.5 (16)	6.5 ± 0.3 (16)	2.7 ± 0.2 (10)
R_q	3.6 ± 0.2	3.5 ± 0.4	3.4 ± 0.4	3.1 ± 0.4	2.8 ± 0.2	2.7 ± 0.2	2.5 ± 0.1	3.7 ± 0.4

^a Values for K_q are expressed as M^{-1} . Data are presented as mean \pm SD. Number of experiments is in parentheses. R_q is the ratio $K_q(\text{I}^-)/K_q(\text{Cs}^+)$. Enzyme was incubated with P_i at 25 °C, in the presence of 0.5 mM EGTA. Where indicated, Ca^{2+} was added after fluorescence had been measured with P_i and the quencher. See text for more details.

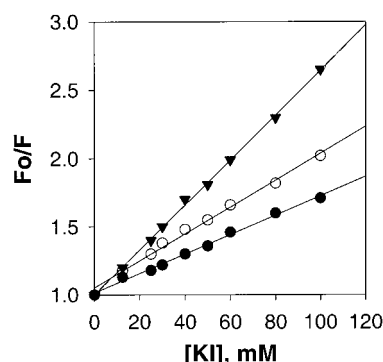


FIGURE 3: Effect of phosphorylation and dephosphorylation on the quenching of FITC-PMCA by KI. The curves represent the data obtained in the presence of 0.5 mM EGTA and 10 mM P_i (▼) and the same points after addition of CaCl_2 to give 100 μM free Ca^{2+} (○). For comparison, the data obtained without P_i but with 100 μM free Ca^{2+} (●) are shown. Basic medium was as in previous figures.

with a higher affinity, binds to the enzyme locking it at a stable nonphosphorylated transition state where the analogue is tetrahedrally coordinated. Structural differences between the phosphate- and vanadate-enzyme complexes have already been suggested by Hua et al. (36) on the basis of the different degrees of protection afforded by vanadate and phosphate against derivatization of SERCA by ThioGlo1. Here we show that the $\text{E}_2 \cdot \text{VO}_4$ state seems to hinder the FITC molecule as much as the binding of Ca^{2+} does. This may be interpreted as if a more “closed” state of the nucleotide site or its surroundings is assumed on the transition state for phosphoryl transfer during the forward PMCA cycle (or conversely for phosphorylation by P_i on the reverse cycle). Yet again, as the ionization state of orthovanadate would be similar to that of phosphate, the different K_q values observed for both ligands would preclude a major charge effect of either P_i or vanadate on the K_q for both KI and CsCl.

DISCUSSION

In this work we studied the quenching of fluorescence of FITC bound to PMCA stabilized in different conformations according to the composition of the medium. In contrast to the data reported by Highsmith (31) for the membranous SERCA, the quenching of FITC-PMCA by both I^- and Cs^+ had the characteristics of static quenching. Static quenching components must mean that there is a finite probability that the quencher exists near a fluorescein residue at the instance of excitation (32). This may occur either by binding of the quencher to the fluorophore or by a relatively long permanence of the quencher near the fluorophore (into what is called “the active volume”). Because the same effects were

observed with quenchers of opposite charge and because the conformational changes of the PMCA modify the values of K_q for both quenchers in the same direction, the most likely mechanism for the quenching would be the entrapping of quencher molecules homogeneously dissolved in water into a pocket containing the FITC bound to Lys-591. The time of permanence of the quenchers in this pocket would depend on the velocities of exchange with the bulk medium and, thus, to medium accessibility.

Our results show that the ligand-induced changes of the quenching constants, and thus in the accessibility of the FITC (bound to Lys-591) to the solvent, are large enough to be accurately measured and show that, independently of the charge of the quencher, the K_q values observed for the conformational states of the PMCA ultimately vary in the same order, which is $\text{E}_1 \cdot \text{Ca} \cdot \text{CaM} < \text{E}_2 \cdot \text{VO}_4 \leq \text{E}_1 \cdot \text{Ca} < \text{E}_2 < \text{E}_2 \text{P}$. These results, although obtained in equilibrium and not when the enzyme is cycling, probably represent appropriately the conformational information of the site where the FITC molecule is inserted, and thus its water accessibility, during the catalytic cycle of the PMCA. Many kinetic properties, such as the impeding of binding, hydrolysis, and phosphorylation by ATP, paralleled by the preservation of phosphorylation by P_i and/or hydrolysis of small pseudosubstrates, were observed for either the Na^+, K^+ -ATPase (29), SERCA (28), H^+ -ATPase (37), or the PMCA itself (30) and give support to the proposal that FITC might be indeed bound to a lysine residue located within or in the near vicinity of the nucleotide domain of the catalytic site of various P-type ATPases. Therefore, one might be tempted to believe that the results presented here are good estimates of the changes in hydration that the catalytic site would undergo during substrate hydrolysis. If this is true, then our data clearly indicate that water accessibility to the nucleotide domain is diminished when the enzyme binds Ca^{2+} , prior to ATP binding by the E_1 state. On the other hand, the K_q values observed when the enzyme is phosphorylated by P_i clearly indicate a much higher accessibility to water in the $\text{E}_2 \cdot \text{P}$ state. These data are also in contrast to the results reported by Highsmith (31) for the membranous SERCA. In that case, the binding of Ca^{2+} induced a decrease in the fluorescence intensity and increased collisional quenching by I^- , evidencing an increase in water accessibility of the fluorophore, whereas phosphorylation by P_i increased the fluorescence yield and decreased the quenching constants, thus indicating that the $\text{E}_2 \cdot \text{P}$ conformation had a more hydrophobic characteristic at the nucleotide site. This apparent dichotomy could be related to differences in the catalytic mechanism of either enzyme for substrate hydrolysis. Hence, phosphoenzyme hydrolysis is defined as the rate-limiting step of the SERCA reaction cycle, with a dephosphorylation rate of

$\sim 3.4\text{--}20\text{ s}^{-1}$ at 25°C (38, 39), whereas the rate measured for the PMCA is at least 1 order of magnitude greater, with a rate constant of 125 s^{-1} at 37°C (40). This could be interpreted as if the rate of phosphoenzyme hydrolysis could be directly influenced by the amount of water surrounding the catalytic site, therefore facilitating this reaction. Coincidentally, the rate of phosphoenzyme hydrolysis of the Na^+, K^+ -ATPase is also in the (fast) range of $200\text{--}366\text{ s}^{-1}$ at room temperature (41, 42), and in parallel the fluorescence of FITC bound to Na^+, K^+ -ATPase was shown to decrease for the phosphoenzyme, as well as for the $\text{E}_2\cdot\text{K}$ and $\text{E}_2\cdot\text{K}\cdot\text{Mg}$ forms, therefore suggesting a more polar (water accessible?) environment for the nucleotide site on the E_2 conformer (43) that could thus enhance the rate of phosphoenzyme hydrolysis. However, whether fluorescence quenching was indeed due to water exposure or to interactions of local charges with the FITC molecule at the binding site of the Na^+, K^+ -ATPase could not be distinguished by those authors.

A remark should be made with regard to the fact that usually the ratio $K_q(\text{I}^-)/K_q(\text{Cs}^+)$ (R_q) was roughly between 2.5 and 3.6 except for the $\text{E}_1\cdot\text{Ca}^{2+}$ and $\text{E}_1\cdot\text{Ca}^{2+}\cdot\text{CaM}$ states, for which this ratio increased to 6.3 and 9.6. Despite the intrinsic fact of I^- being a more potent quencher than Cs^+ , this increase in the ratio could imply that upon the binding of Ca^{2+} , a cluster of positive charges could be exposed, therefore enhancing quenching by I^- through electrostatic attraction. This observation would be in conformity with the structural data obtained from the primary structure and X-ray crystallography of SERCA (44), which clearly show an array of basic amino acids surrounding the nucleotide cleft of the enzyme. By analogy, and on the basis of the increase of the R_q , one would presume that such a cluster could also be present on the catalytic site of PMCA and might be involved in coordinating and positioning the adenosine moiety and the triphosphate group of ATP for catalysis and phosphoryl transfer to the enzyme.

The variation in K_q values induced by phosphorylation of the FITC-PMCA with P_i are a strong indication that for the $\text{E}_2\cdot\text{P}$ conformer the bound FITC is more accessible to quenchers than in any other state studied. As K_q was greatly increased for both quenchers, this is interpreted as representing a much higher solvent accessibility of this site in the phosphorylated state. It is noteworthy that this is opposite that observed for SERCA (31). For SERCA and other P-type ATPases it has been suggested, using a variety of techniques (44–46), that the catalytic site is in a more “closed” state in the $\text{E}_2\cdot\text{P}$ conformation than in the dephosphorylated conformers.

Our data also report the affinity for P_i of the PMCA. Our results show that for both quenchers, the apparent K_m for phosphate is $\sim 2\text{ mM}$ ($1.58/2.63\text{ mM}$ as determined using I^- or Cs^+ , respectively). To our knowledge, this is the first direct report of the affinity for inorganic phosphate of the erythrocyte PMCA and reveals that, as expected, the affinity is in the millimolar range as for other P-type ATPases. Furthermore, the addition of Ca^{2+} to the phosphorylated enzyme is still able to induce dephosphorylation, as indicated by the decrease in the K_q values observed upon addition of the ion, supporting the assumption that the labeled enzyme is still competent in terms of response to ligand binding and catalysis. For instance, these results are also an indication

of the sensitivity and reliability of the use of FITC-PMCA with KI and CsCl as fluorescence quenchers for detecting both the conformational changes of the enzyme and the accessibility of the catalytic site.

High levels of K^+ reduce the amount of phosphoenzyme formed by P_i in most P-type ATPases (47, 48). For the PMCA, the effects of K^+ in the phosphoenzyme levels are not well characterized. Herscher et al. (49) reported that K^+ increases the steady state levels of phosphoenzyme formed by ATP, an effect that is also opposite what is described for other P-type ATPases (50). Because the data in Figure 2 were obtained in the presence of high concentrations of K^+ , an alternative possibility might be that, in our experiments, the non-covalent adduct $\text{E}_2\cdot\text{P}$ had accumulated, instead of the phosphoenzyme $\text{E}_2\cdot\text{P}$. However, such a hypothesis is rather unlikely, because the conformer accumulated in Figure 2 displayed K_q values for I^- and Cs^+ opposite that observed for the supposedly analogous adduct $\text{E}_2\cdot\text{VO}_4$ (see Table 1).

When the enzyme was locked at a transitional state by the phosphate analogue orthovanadate, the K_q values decreased to relatively low values that might be interpreted as a strong dehydration of the nucleotide site on the transitional state. As K_q increased again for the ligand-free EGTA medium, which theoretically induced a free $\text{E}_2\text{--E}_1$ equilibrium (see Tables 1 and 3), the results might represent that dephosphorylation of the E_2 conformer of PMCA involves sequential intermediate steps of hydration (at $\text{E}_2\cdot\text{P}$), dehydration when hydrolysis of the phosphoenzyme occurs, with a solvent-shielded catalytic site (represented by the vanadate-induced state), and rehydration for the release of the phosphate molecule to the aqueous media (at an $\text{E}_2\cdot\text{P} \leftrightarrow \text{E}_2$ step). Furthermore, the low solvent accessibility of the $\text{E}_1\cdot\text{Ca}\cdot\text{CaM}$ and $\text{E}_1\cdot\text{Ca}$ states might be in consonance with the reaction of the γ -phosphoryl group transfer from ATP to the enzyme, where a less hydrated, yet polar (due to the basic amino acid cluster on the E_1 state), catalytic site could facilitate the phosphate transfer to the aspartyl residue phosphorylated on the P-type ATPases during the forward cycle and, conversely, facilitate the reverse reaction of phosphorylation by P_i in the reverse cycle (51, 52). Although this last topic of discussion is very speculative, our results support these hydration/accessibility/polarity changes on the nucleotide site of the FITC-PMCA, thus suggesting that these aspects of PMCA are distinct from the observed for other P-type ATPases and may therefore explain some of the kinetic differences between these enzymes.

ACKNOWLEDGMENT

We gratefully acknowledge the technical assistance of Rita C. Q. Figueira and Rosângela R. Ferreira in preparing ghosts and purified PMCA and FITC-PMCA. We especially thank Dr. Adalberto R. Vieyra for kindly allowing the use of the Hitachi F-4500 fluorometer used in this work and Dr. Carlos S. Bonafé and FAPESP for permitting the use of the Edinburgh OB920 fluorescence lifetime spectrometer.

REFERENCES

1. Carafoli, E., and Guerini, D. (1993) *Trends Cardiovasc. Med.* 3, 177–184.
2. Carafoli, E., and Brini, M. (2000) *Curr. Opin. Chem. Biol.* 4, 152–161.

3. Verma, A. K., and Penniston, J. T. (1984) *Biochemistry* 23, 5010–5015.
4. Pedersen, P. H., and Carafoli, E. (1987) *Trends Biochem. Sci.* 12, 186–189.
5. Niggli, V., Adunyah, E. S., Penniston, J. T., and Carafoli, E. (1981) *J. Biol. Chem.* 256, 395–401.
6. Carafoli, E. (1994) *FASEB J.* 8, 993–1002.
7. Kosk-Kosicka, D., Bzdega, T., and Wawrzynow, A. (1989) *J. Biol. Chem.* 264, 19495–19499.
8. Vorherr, T., Kessler, T., Hoffman, F., and Carafoli, E. (1991) *J. Biol. Chem.* 266, 22–27.
9. Enyedi, A., Sarkadi, B., Szaz, I., Bot, B., and Gardos, G. (1980) *Cell Calcium* 1, 299–310.
10. Niggli, V., Adunyah, E. S., Penniston, J. T., and Carafoli, E. (1981) *J. Biol. Chem.* 256, 395–401.
11. Wang, K. K. W., Wright, L. C., Machan, C. L., Allen, B. G., Conigrave, A. D., and Roufogalis, B. D. (1991) *J. Biol. Chem.* 266, 9078–9085.
12. Enyedi, A., Verma, A. K., Filoteo, A. G., and Penniston, J. T. (1996) *J. Biol. Chem.* 271, 32461–32466.
13. Penniston, J. T., and Enyedi, A. (1998) *J. Membr. Biol.* 165, 101–109.
14. Garrahan, P. J. (1986) in *The Ca^{2+} Pump of Plasma Membranes: Partial Reactions of the Ca^{2+} -ATPase* (Rega, A. F., and Garrahan, P. J., Eds.) CRC Press, Boca Raton, FL.
15. Carafoli, E., Garcia-Martin, E., and Guerini, D. (1996) *Experientia* 52, 1091–1100.
16. Filoteo, A. G., Gorski, J. P., and Penniston, J. T. (1987) *J. Biol. Chem.* 262, 6526–6530.
17. Walseth, T. F., and Johnson, R. A. (1979) *Biochim. Biophys. Acta* 562, 11–31.
18. Rega, A. F., Garrahan, P. J., Barrabin, H., Horenstein, A., and Rossi, J. P. (1979) in *Cation Flux Across Biomembranes* (Mukohata, Y., and Packer, L. Eds.) pp 67–76, Academic Press, New York.
19. Caroni, P., Zurini, M., Clark, A., and Carafoli, E. (1983) *J. Biol. Chem.* 258, 7305–7310.
20. Pasa, T. B. C., Otero, A. S., Barrabin, H., and Scofano, H. M. (1992) *J. Mol. Cell. Cardiol.* 24, 233–242.
21. Lowry, O. H., Rosenbrough, N. Y., Farr, A. L., and Randall, R. J. (1951) *J. Biol. Chem.* 193, 265–275.
22. Peterson, G. L. (1977) *Anal. Biochem.* 83, 346–356.
23. Carvalho-Alves, P. C., and Scofano, H. M. (1987) *J. Biol. Chem.* 262, 6610–6614.
24. Sorenson, M. M., Coelho, H. S. L., and Reuben, J. P. (1986) *J. Membr. Biol.* 90, 219–230.
25. Fabiato, A., and Fabiato, F. (1979) *J. Physiol. (Paris)* 75, 463–505.
26. Schwarzenbach, G., Senn, H., and Anderegg, G. (1957) *Helv. Chim. Acta* 40, 1886–1900.
27. Eftink, M. R. (1983) in *Principles of Fluorescence—Fluorescence Quenching: Theory and Applications* (Lakowicz, J. R., Ed.) Plenum Publishing, New York.
28. Pick, U., and Bassilian, S. (1981) *FEBS Lett.* 123, 127–130.
29. Davis, R. L., and Robinson, J. D. (1988) *Biochim. Biophys. Acta* 953, 26–36.
30. Donnet, C., Caride, A. J., Talgham, S., and Rossi, J. P. F. C. (1998) *J. Membr. Biol.* 163, 217–224.
31. Highsmith, S. (1986) *Biochemistry* 25, 1049–1054.
32. Eftink, M. R. (1991) in *Topics in Fluorescence Spectroscopy* (Lakowicz, J. R., Ed.) pp 53–126, Plenum Press, New York.
33. Chiesi, M., Zurini, M., and Carafoli, E. (1984) *Biochemistry* 23, 2595–2600.
34. Vieyra, A. R., Caruso-Neves, C., and Meyer-Fernandes, J. R. (1991) *J. Biol. Chem.* 266, 10324–10330.
35. de Meis, L., and Vianna, A. L. (1979) *Annu. Rev. Biochem.* 48, 275–292.
36. Hua, S., Fabris, D., and Inesi, G. (1999) *Biophys. J.* 77, 2217–2225.
37. Pardo, J. P., and Slayman, C. W. (1988) *J. Biol. Chem.* 263, 18664–18668.
38. Mignaco, J. A., Barrabin, H., and Scofano, H. M. (1996) *J. Biol. Chem.* 271, 18423–18430.
39. Fujimori, T., and Jencks, W. P. (1992) *J. Biol. Chem.* 267, 18466–18474.
40. Herscher, C. J., Rega, A. F., and Garrahan, P. J. (1994) *J. Biol. Chem.* 269, 10400–10406.
41. Mårdh, S., and Post, R. L. (1977) *J. Biol. Chem.* 252, 633–638.
42. Kane, D. J., Grell, E., Bamberg, E., and Clarke, R. J. (1998) *Biochemistry* 37, 4581–4591.
43. Hegyvary and Jorgensen (1981) *J. Biol. Chem.* 256, 6296–6303.
44. Toyoshima, C., Nakasako, M., Nomura, H., and Ogawa, H. (2000) *Nature* 405, 647–655.
45. Danko, S., Yamasaki, K., Daiho, T., Suzuki, H., and Toyoshima, C. (2001) *FEBS Lett.* 505, 129–135.
46. Bishop, J. E., Nakamoto, R., and Inesi, G. (1986) *Biochemistry* 25, 696–703.
47. Skou, J. C., and Esmann, M. (1992) *J. Bioenerg. Biomembr.* 24, 249–261.
48. Masuda, H., and de Meis, L. (1973) *Biochemistry* 12, 4581–5585.
49. Herscher, C. J., Rega, A. F., and Adamo, H. (1996) *Biochem. J.* 315, 673–677.
50. Chaloub, R. M., and de Meis, L. (1980) *J. Biol. Chem.* 255, 6168–6172.
51. de Meis, L., and Suzano, V. A. (1988) *FEBS Lett.* 232, 73–77.
52. Benaim, G., and de Meis, L. (1990) *Biochim. Biophys. Acta* 1026, 87–92.

BI015783V